SUPPLEMENTARY MATERIALS AND METHODS

Generation of *Lrp4*^{LacZ}, *Lrp4*$^{\Delta ICD}$, *Lrp4*^{R1170W} mice using the CRISPR/Cas9 technology

For an in-frame insertion of *LacZ* into the first exon of Lrp4, a donor plasmid was generated by capturing the *LacZ-SV40polyA* cassette and flanking regions from the *Lrp4-LacZ* BAC clone (Ahn et al., 2013). The resulting plasmid contains left and right homology arms from the *Lrp4* locus (2.3 kb and 1.0 kb, respectively). Germline transmission of the targeted allele was achieved by crossing a founder with wild-type C57BL/10JxCBA-F1 mice.

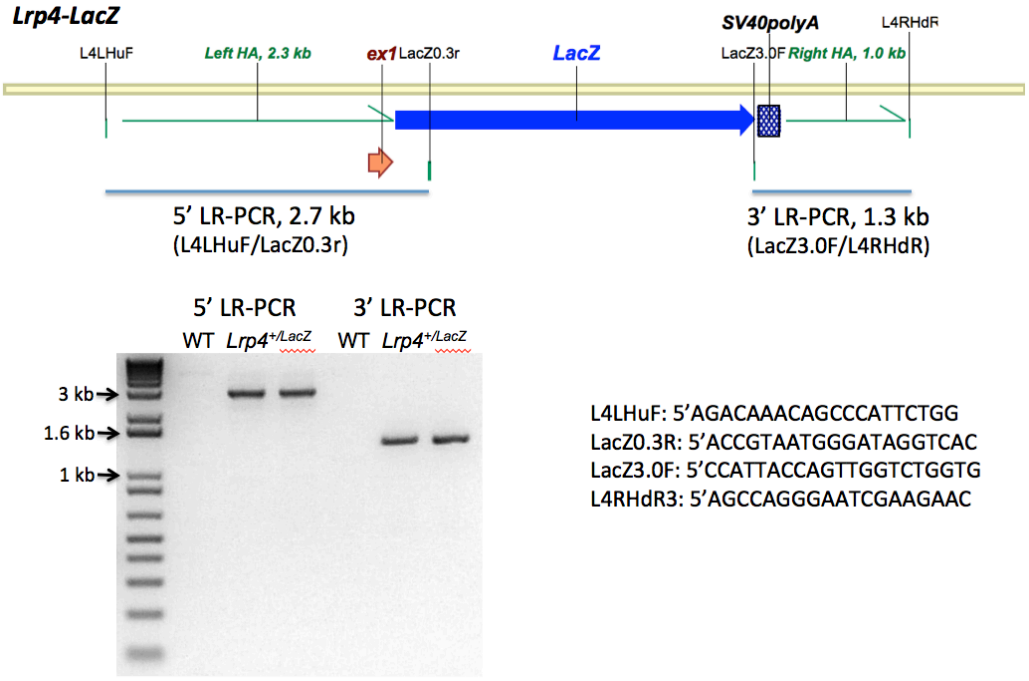

After successful germline transmission, correct targeting was confirmed in mice heterozygous for the *LacZ* knock-in allele (*Lrp4*$^{+/LacZ}$) by long-range PCR with combinations of primers, one of which is external to the homology arms (see the figure above). The strain was maintained as heterozygotes since mice homozygous for the allele are not viable.

Lrp4$^{\Delta ICD}$ and *Lrp4*^{R1170W} mice were generated by co-injecting a pX330 plasmid and an oligo donor with the desired mutation into FVB/N embryos. For each model, two founder mice were bred to wild-type FVB/N mice for germline transmission. Correct targeting was confirmed by PCR amplification and sequencing of the targeted regions from heterozygous mice (see the figure below). Primers used for the PCR are,
Lrp4$^{\Delta ICD}$: 5'-TCCATCTGTCCCCCAGCATC and 5'-CTTTCTCACCCACTCAGGCA
Lrp4^{R1170W}: 5'-GCTCACAGCATGAGGACATC and 5'-TGCTCCTATGCTTCATGGTC

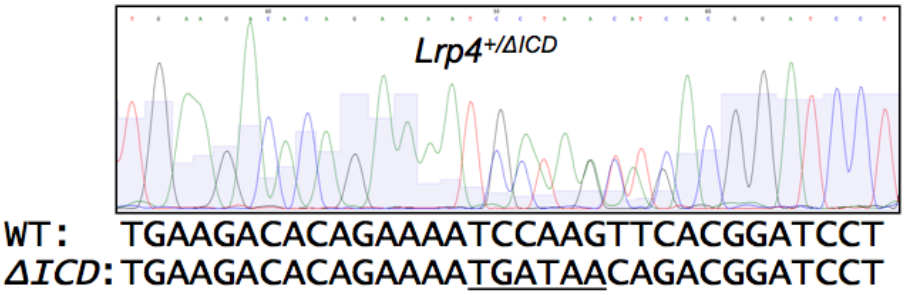

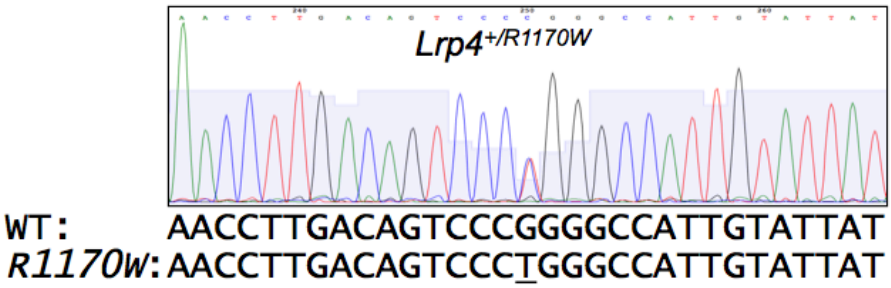

After successful germline transmission, heterozygous mice from individual founders were crossed to generate homozygous mice. Homozygous *Lrp4*$^{\Delta ICD}$ and *Lrp4*^{R1170W} mice are viable and two independent lines with the same mutation display tooth phenotypes indistinguishable from each other.

For generation of the *Lrp4*^{LacZ}, *Lrp4*$^{\Delta ICD}$, *Lrp4*^{R1170W} mice with CRISPR/Cas9 technology, seed sequences were carefully selected to minimize potential risk of off-target effect. Specifically, the selected seed sequences do not have any potential off-target with off-target score over 2.0 (www.benchling.com) across the whole mouse genome.

Ahn, Y., Sims, C., Logue, J.M., Weatherbee, S.D., Krumlauf, R., 2013. Lrp4 and Wise interplay controls the formation and patterning of mammary and other skin appendage placodes by modulating Wnt signaling. Development 140, 583-593.

Supplementary Table S1. Summary of mouse strains used in the study

Gene	Allele	Modification/Purpose	Gene function	Reference
Lrp4	*mitt*	Premature stop codon in exon 10	null	Weatherbee et al., 2006
Lrp4	*mte*	D1436G missense mutation	null	Weatherbee et al., 2006
Lrp4	*LacZ*	*LacZ* insertion into exon 1	null	this study
Lrp4	*ECD*	Insertion of a stop codon before the transmemebrane domain	hypomorphic	Johnson et al., 2005
Lrp4	*mdig*	A point mutations causing skipping of exon 15	hypomorphic	Simon-Chazottes et al., 2006
Lrp4	*R1170W*	R1170W misssense mutation	hypomorphic	this study
Lrp4	*ΔICD*	Insertion of a stop codon after the transmemebrane domain	hypomorphic	this study
Lrp4	*tetO-Lrp4*	Random integration/tTA-dependent over-expression	gain-of-function	this study
Lrp4-Lrp6	*tetO-Lrp4ECDLrp6ICD*	Random integration/tTA-dependent over-expression	gain-of-function	this study
Lrp4	*Lrp4BAC-tTA*	Random integration/tTA expression from an *Lrp4* BAC clone	tTA driver	this study
Lrp5	*null*	Insertion of *IRES-LacZ-Neo* at amino acid 373	null	Kato et al., 2002
Lrp6	*null*	Insertion of *LacZ* at amino acid 321	null	Pinson et al., 2000
Lrp6	*tetO-Lrp6*	Random integration/tTA-dependent over-expression	gain-of-function	this study
Wise	*null*	*LacZ* insertion into exon 1	null	Ahn et al., 2010
Wise	*tetO-Wise*	Random integration/tTA-dependent over-expression	gain-of-function	Ahn et al., 2013
KRT14	*K14-tTA*	Random integration/tTA expression driven by a human *KRT14* promoter	tTA driver	Ahn et al., 2013

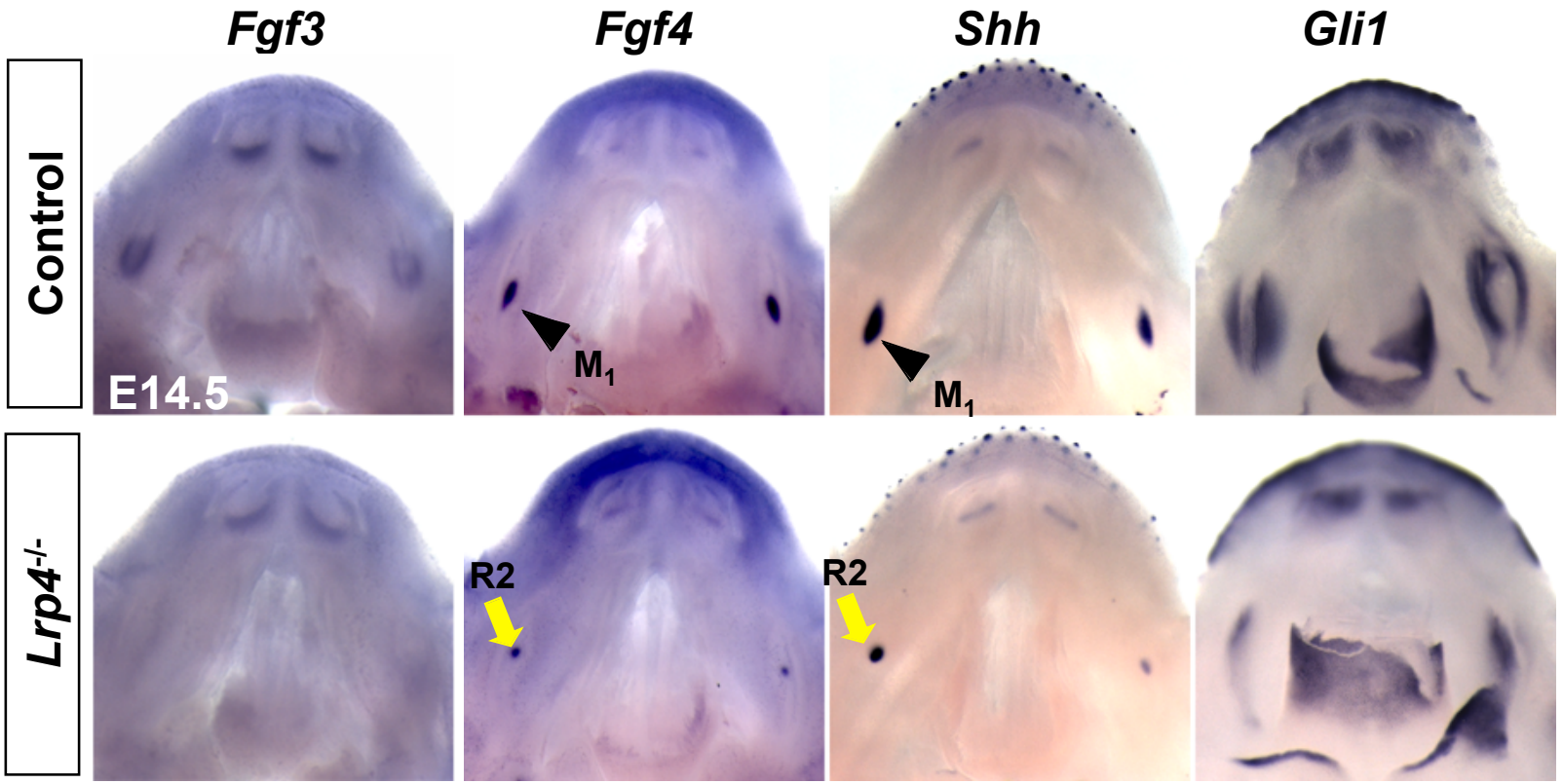

Suppl. Fig. S1. Abnormal embryonic tooth development in *Lrp4*-null mice.

Differential gene expression at E14.5 in the tooth germ of *Lrp4*-null mice shown by *in situ* hybridization with mandibles. Control mice are wild-type or heterozygous for either $Lrp4^{mitt}$ or $Lrp4^{mte}$ allele and $Lrp4^{-/-}$ mice are homozygous for either $Lrp4^{mitt}$ or $Lrp4^{mte}$ allele.

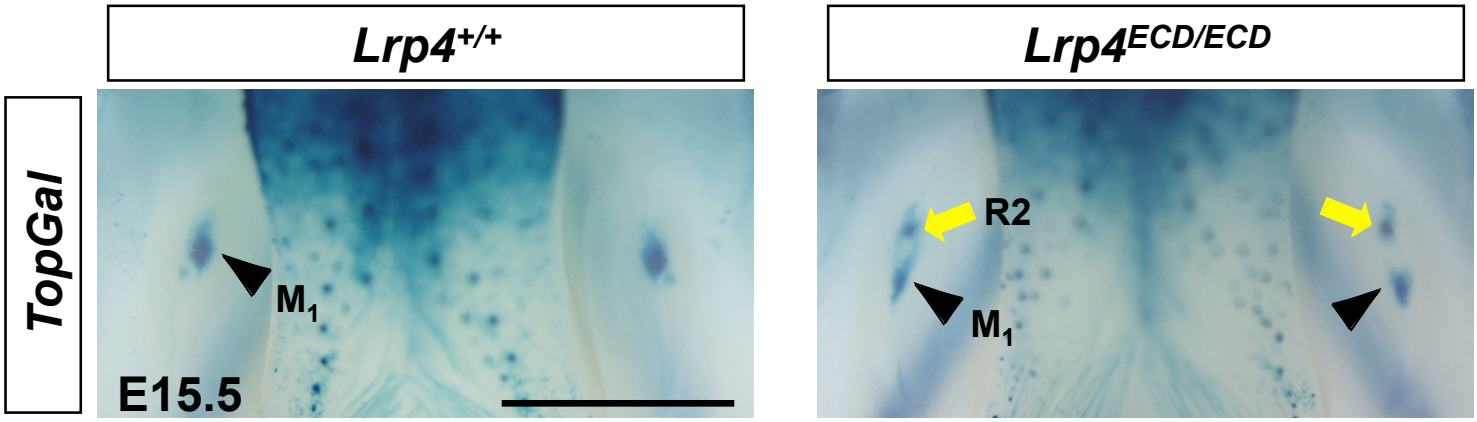

Suppl. Fig. S2. Abnormal *TopGal* expression pattern in teeth of *Lrp4*$^{ECD/ECD}$ mice.

TopGal staining indicates that R2 gives rise to a supernumerary tooth in *Lrp4*$^{ECD/ECD}$ mice. Similar to *Lrp4*-null mice, these mice display variable distance between R2 and M_1. Scale bar 1 mm.

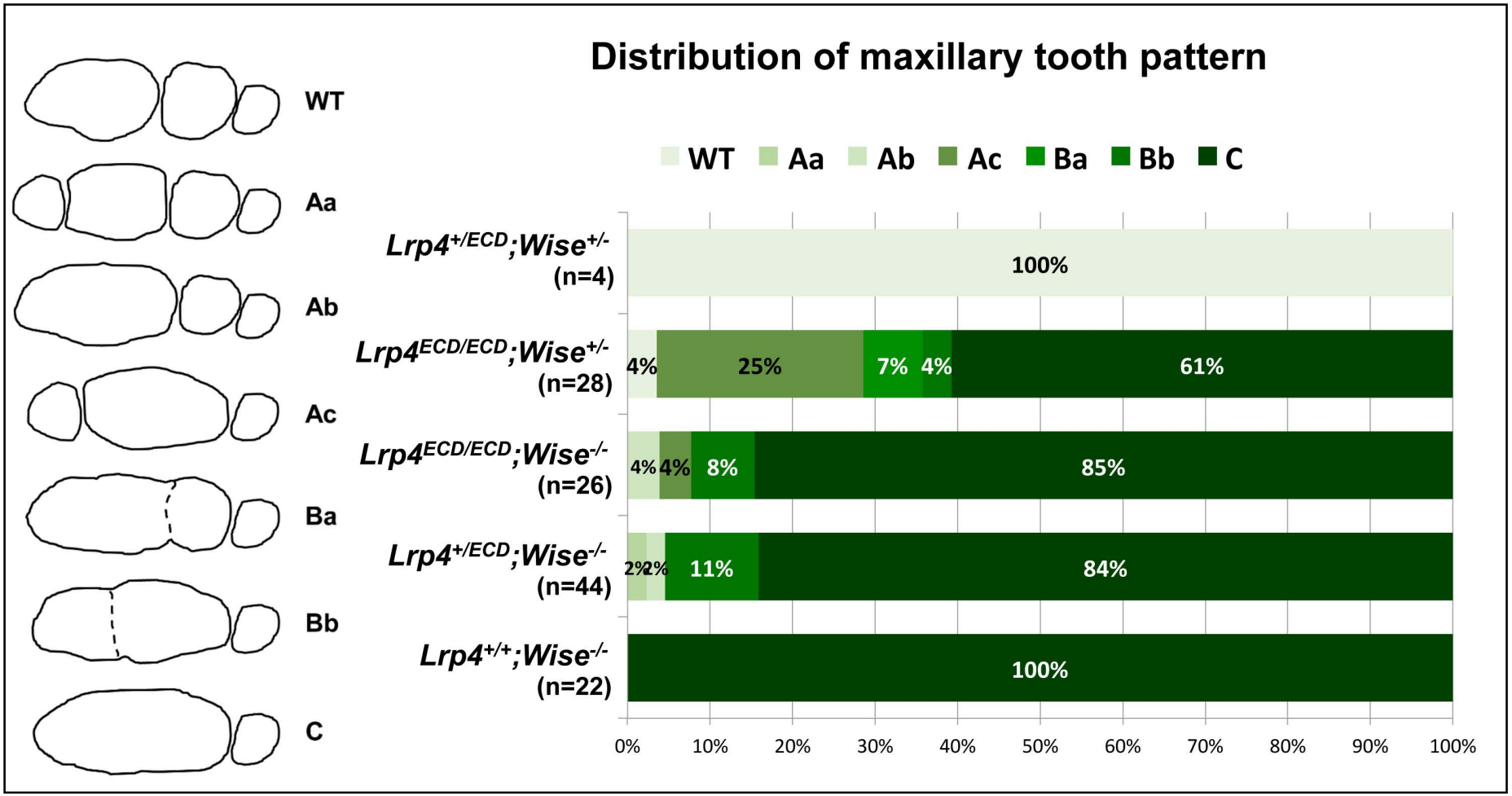

Suppl. Fig. S3. *Lrp4* deficiency ameliorates *Wise*-null tooth defects in the maxilla.

Maxillary tooth patterns are categorized based on the number, size and fusion of cheek teeth (left). Distribution of different tooth patterns among littermates of the $Lrp4^{ECD}$ and *Wise*-null combinatorial mutants (right).

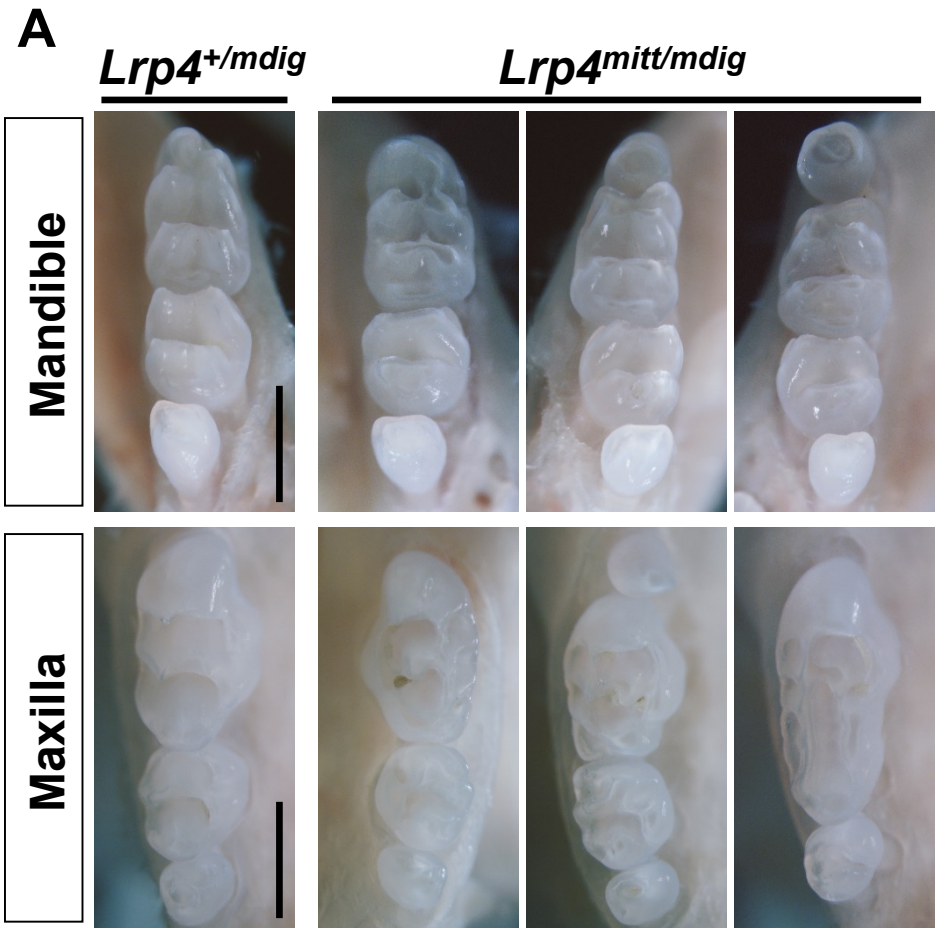

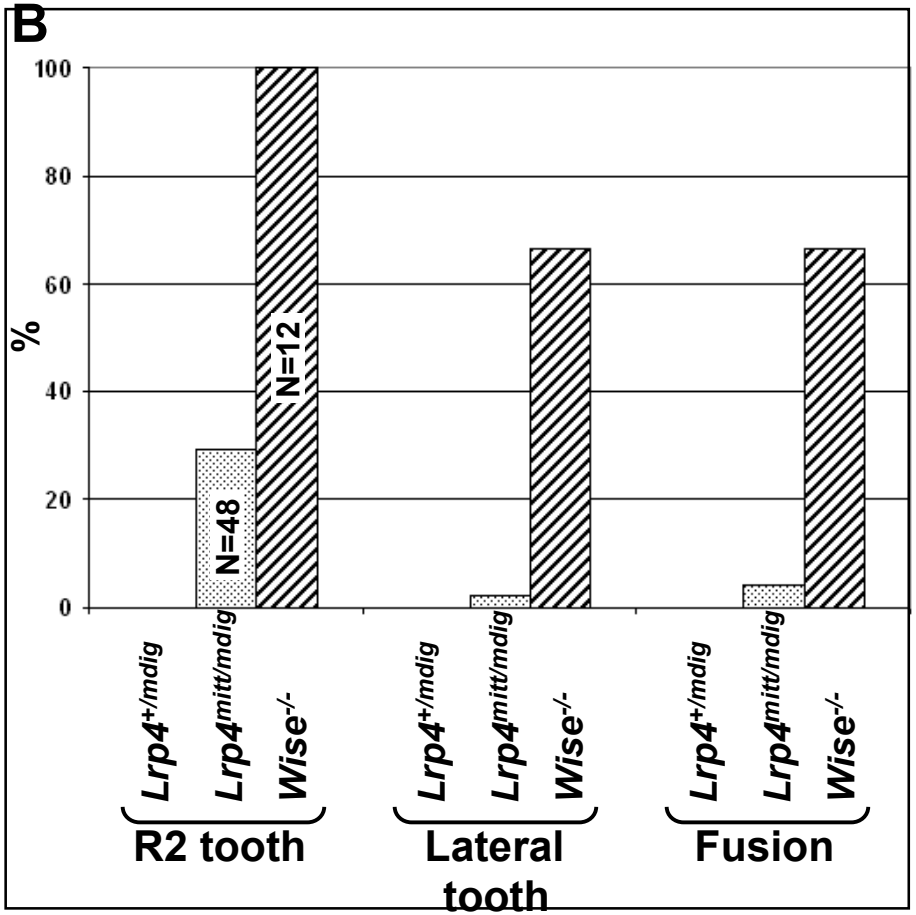

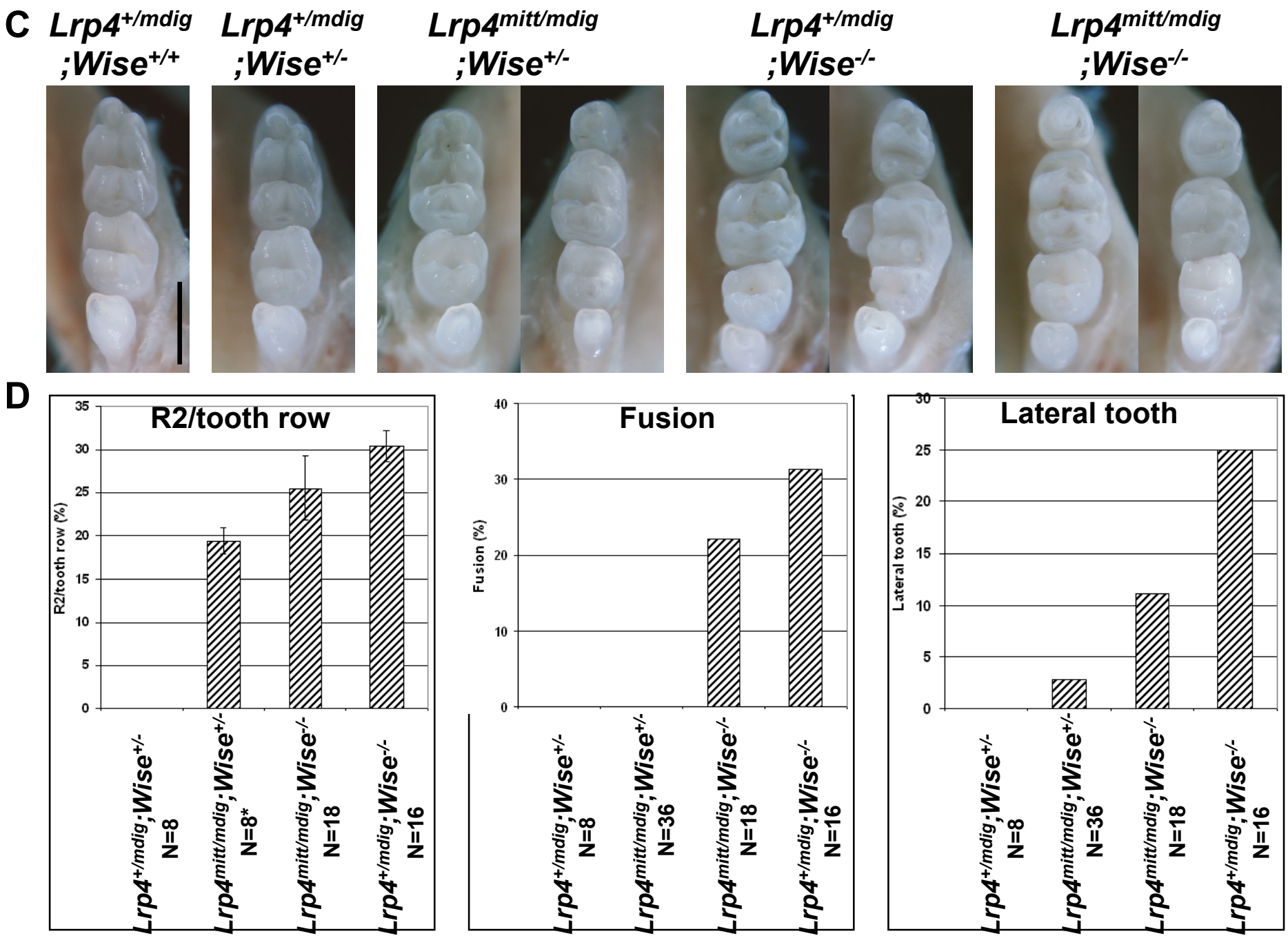

Suppl. Fig. S4. *Lrp4* deficiency ameliorates *Wise*-null tooth defects.

(A) Representative tooth patterns of *Lrp4*$^{mitt/mdig}$ mice.
(B) *Lrp4*$^{mitt/mdig}$ mice display variable, but generally milder tooth defects in the mandible compared to *Wise*-null mice.
(C) Representative tooth patterns of *Lrp4* and *Wise* combinatorial mutants.
(D) *Lrp4* deficiency ameliorates tooth defects of *Wise*-null mice in a dose dependent manner in the mandible. Relative size of R2 (left) and frequency of molar fusion (middle) and lateral supernumerary teeth (right) per jaw quadrant were scored among littermates. *: only 8 quadrants with a R2 tooth were scored and the others (28) had the normal three-molar pattern.
Scale bar 1 mm.

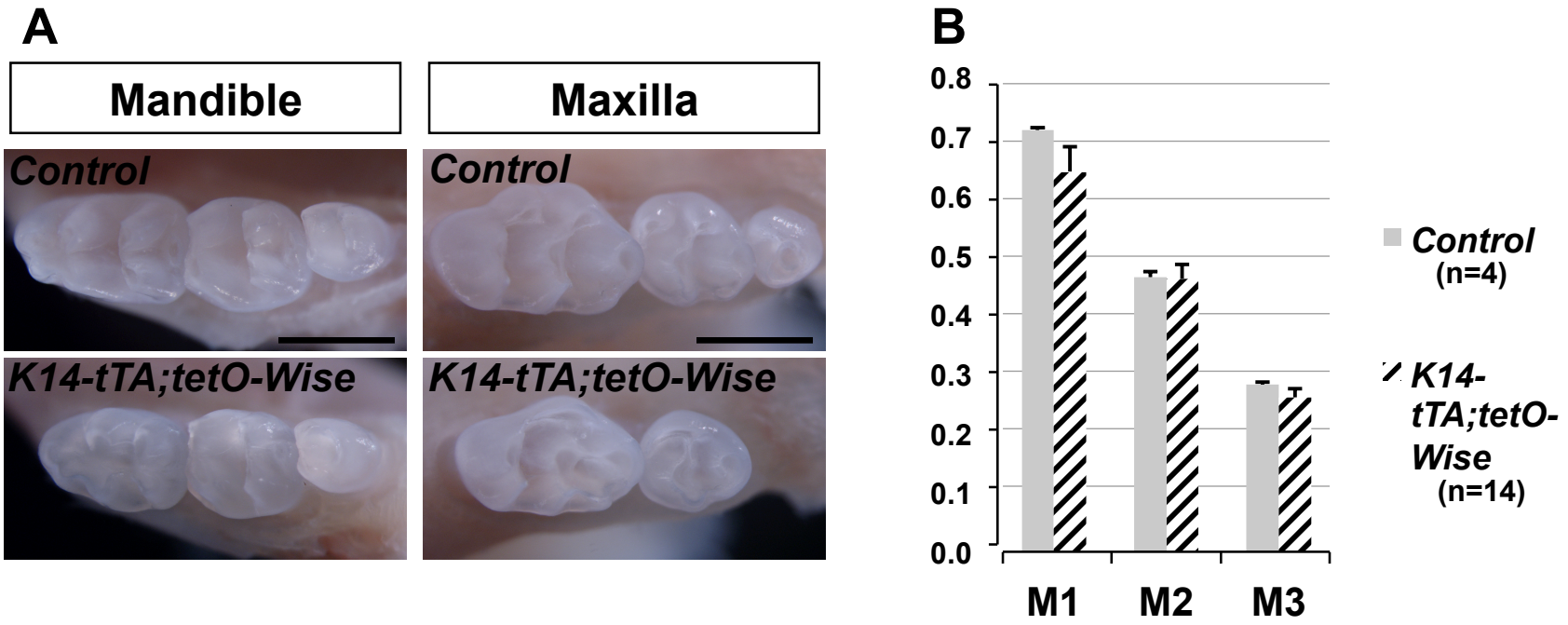

Suppl. Fig. S5. *Wise* over-expression disrupts tooth development.

(A) Molars are generally smaller and in the maxilla M_3 is often missing (28.6%, 4/14) in *K14-tTA;tetO-Wise* mice. Scale bar 1 mm.
(B) Mandibular M_1 and M_3 are significantly smaller in *K14-tTA;tetO-Wise* mice (M_1: p=0.0036; M_3: p=0.045) while M_2 are similar in size. Error bar: standard deviation

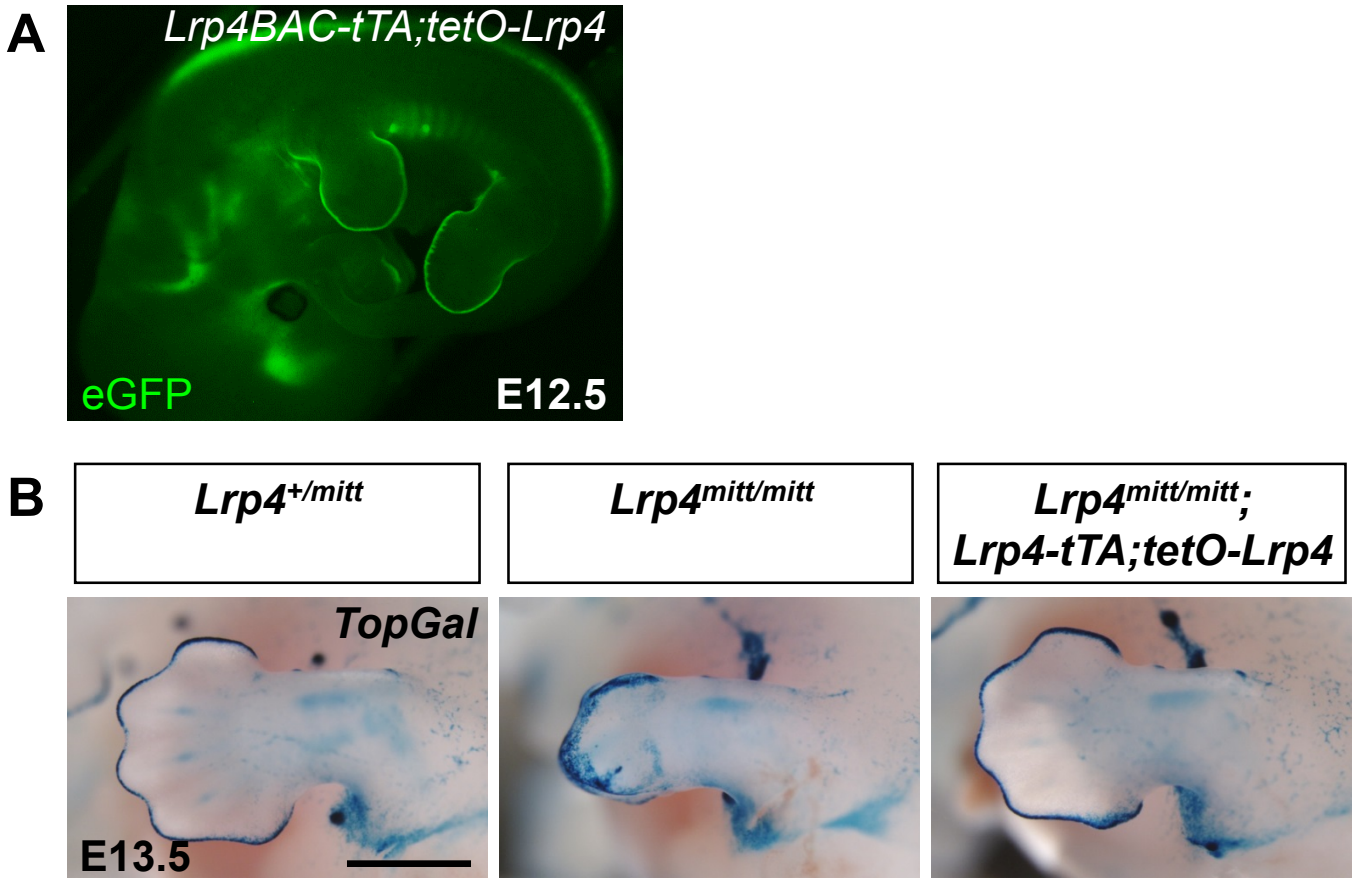

Suppl. Fig. S6. Transgenic *Lrp4* expression rescues *Lrp4*-null limb defect.

(A) eGFP expression driven by *Lrp4* BAC-tTA transgene which recapitulates the endogenous *Lrp4* expression pattern in the limb buds.
(B) *TopGal* expression indicates abnormal patterning of the distal limb in $Lrp4^{mitt/mitt}$ mice is rescued by transgenic *Lrp4* expression.
Scale bar 1 mm.

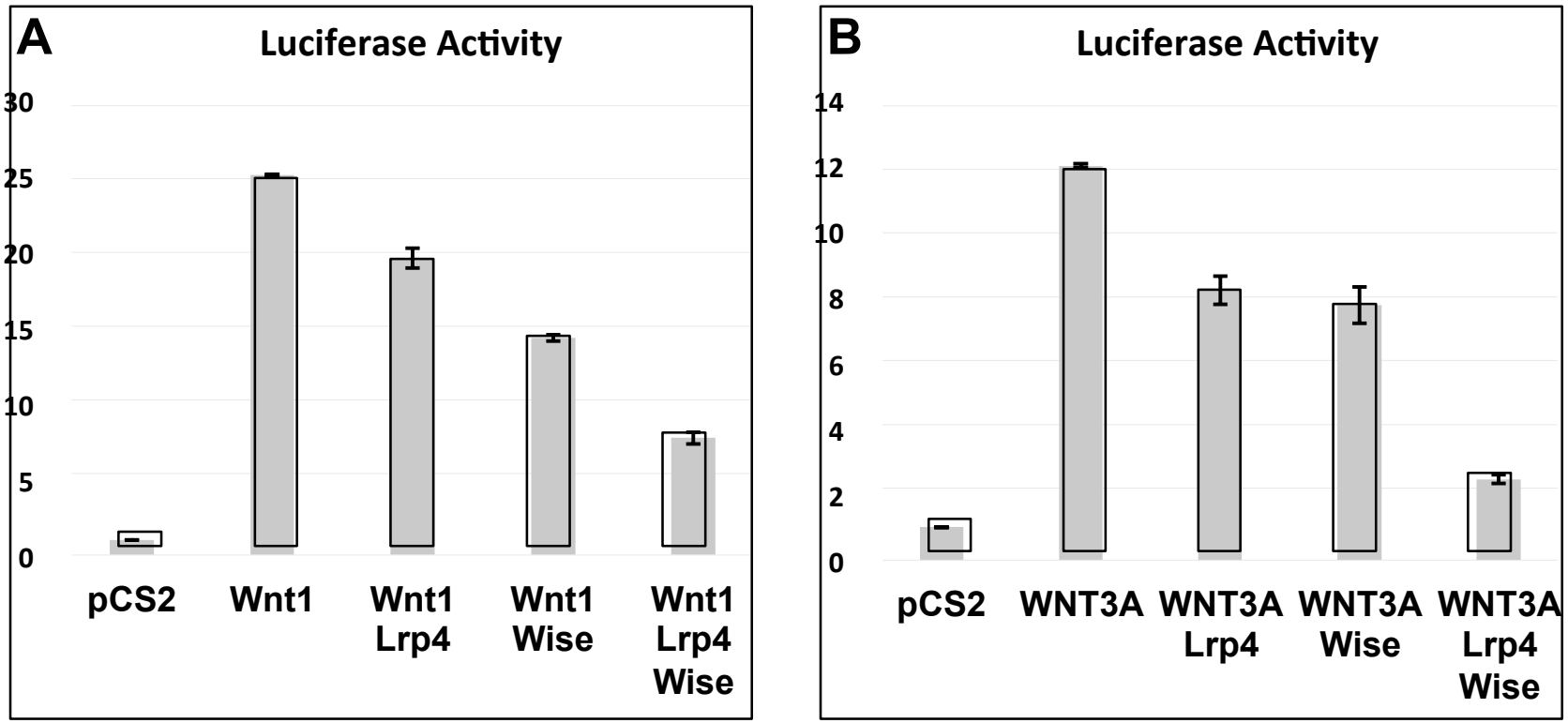

Suppl. Fig. S7. *Lrp4* and *Wise* cooperatively inhibit Wnt/β-catenin signaling *in vitro*.

(A) Relative luciferase activity from TOPflash reporter activated by Wnt1. HEK 293T cells were transfected with an empty vector (pCS2) or constructs driving expression of Lrp4 or Wise.
(B) Relative luciferase activity from TOPflash reporter activated by WNT3A.

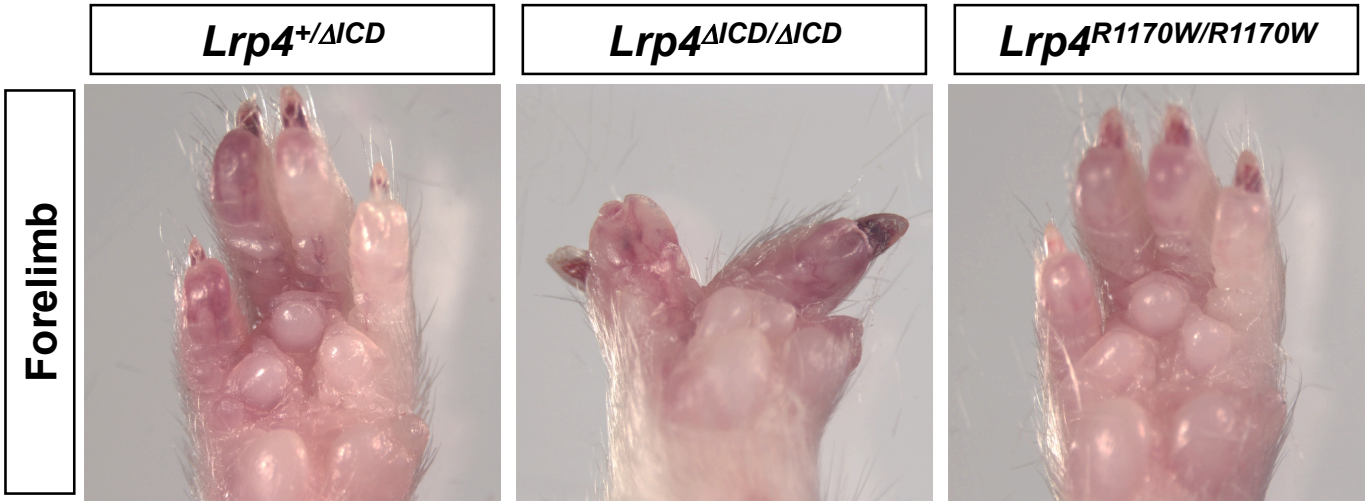

Suppl. Fig. S8. Limb phenotypes of *Lrp4*$^{\Delta ICD/\Delta ICD}$ and *Lrp4*$^{R1170W/R1170W}$ mice.

While the intracellular domain is essential for distal limb patterning (middle), the R1170W mutation does not have significant effect on limb patterning (right).